

(1976).

⁶A. J. Pawlicki *et al.*, Phys. Rev. D **15**, 3196 (1977).⁷D. Cohen *et al.*, Phys. Rev. D (to be published).⁸A. D. Martin and E. N. Ozmutlu, Nucl. Phys. **B158**, 520 (1979).⁹R. H. Dalitz and R. G. Moorhouse, Proc. Roy. Soc., Ser. A **318**, 279 (1970).¹⁰P. Estabrooks and A. D. Martin, Nucl. Phys. **B95**, 322 (1975).¹¹A. D. Martin and M. R. Pennington, Ann. Phys. (N.Y.) **114**, 1 (1978).¹²H. Becker *et al.*, Nucl. Phys. **B151**, 46 (1979); the phase shifts shown in Fig. 3(a) are derived from an average of the g_s and h_s amplitude phases reported by them.¹³P. W. Coulter, Phys. Rev. Lett. **29**, 450 (1972), and Phys. Rev. D **7**, 7 (1973). Coulter's formalism implies Eq. (2) as well as Eq. (3).

Dynamic Influence of Valence Neutrons upon the Complete Fusion of Massive Nuclei

M. Beckerman, M. Salomaa, A. Sperduto,^(a) H. Enge, J. Ball, A. DiRienzo, S. Gazes,
Yan Chen,^(b) J. D. Molitoris, and Mao Nai-feng^(b)

Laboratory for Nuclear Science, Massachusetts Institute of Technology, Cambridge, Massachusetts 02139

(Received 14 May 1980)

Excitation functions for complete fusion of $^{58}\text{Ni} + ^{58}\text{Ni}$, $^{58}\text{Ni} + ^{64}\text{Ni}$, and $^{64}\text{Ni} + ^{64}\text{Ni}$ have been determined over a range of energies from just above to well below the fusion barrier. The response of these excitation functions to the addition of valence neutrons is found to be surprisingly complex. We suggest that at least part of the observed variations may be due to dynamic, single-particle effects.

PACS numbers: 25.70.Bc, 21.60.Cs

Measurements of cross sections for complete fusion at near-barrier and subbarrier energies provide basic information on the large-scale behavior of nuclear matter and on the influence upon this behavior of the underlying nuclear structure. In addition to providing data for testing various interaction potentials and probing (in principle) the nuclear potential at the inner side of the interaction barrier, such measurements may provide insight into a number of predicted static and dynamic aspects. Theoretical predictions which have been made include the occurrence of Coulomb distortions, rotations, and the excitation of vibrational states,¹⁻³ of quantal oscillations,⁴ and the influence of nuclear stiffness⁵ and static deformations.⁶ Recent experimental investigations,⁷⁻⁹ involving ^{16}O to ^{40}Ca projectiles, have revealed the presence of substantial subbarrier penetration. These data have been used to test for the predicted influence of static deformations with suggestive, although somewhat inconclusive, results.^{10,11}

In this Letter we present results of measurements of complete-fusion excitation functions for $^{58}\text{Ni} + ^{58}\text{Ni}$, $^{58}\text{Ni} + ^{64}\text{Ni}$, and $^{64}\text{Ni} + ^{64}\text{Ni}$ at near-barrier and subbarrier energies. These Ni systems involve more massive projectiles than used previously and comprise a triad of massive, nearly closed-shell symmetric, target-projectile combinations. We find that the response of the Ni-Ni

excitation functions to the addition of valence neutrons is complex, more so than observed in systems involving lighter projectiles. We then suggest that at least part of the observed variations may be due to dynamic, single-particle effects.

In order to determine the excitation functions we measured evaporation residue differential cross sections using the Massachusetts Institute of Technology-Brookhaven National Laboratory (MIT-BNL) velocity selector together with a gas ΔE - E telescope. The use of a velocity selector¹² makes possible the high-precision, near-barrier and subbarrier measurements which cannot be made by systems which are limited by the intense elastic scattering from going to sufficiently forward scattering angles. The experiments were performed using 187-220-MeV ^{58}Ni and 171-215-MeV ^{64}Ni beams provided by the BNL Tandem Van de Graaff Facility to bombard isotopically enriched 70-225- $\mu\text{g}/\text{cm}^2$ ^{58}Ni and ^{64}Ni targets.

Two silicon surface-barrier detectors placed at 22° angles to the beam axis were used for beam monitoring and normalization. The velocity selector system consisted of a quadrupole doublet, an electrostatic deflector, the velocity selector proper, and a second quadrupole doublet. The gas ΔE - E telescope was placed at the image of the second quadrupole. The ΔE section consisted of a proportional chamber containing isobutane at 20 mm Hg and the E counter was a 450

mm² silicon surface-barrier detector. Absolute cross sections were obtained by calibrating with Rutherford scattering of 80–120-MeV ¹²⁷I ions from 90–170-μg/cm² Au targets. This technique used ions of similar *Z*, *A*, and kinetic energy as the evaporation residues to determine the corresponding peak absolute efficiencies, thereby automatically taking into account effects of departures of the mean charge states from those presumed and effects of chromatic aberrations. The calibration procedure and experimental uncertainties are discussed in detail in a separate publication.¹³

Evaporation residue angular distributions were measured over angular ranges from 0° to 6° in 1° steps at representative bombarding energies and recoil kinetic-energy spectra were measured at representative recoil angles and bombarding energies with use of calibration-determined velocity-selector field settings. The resulting complete-fusion excitation functions are displayed in Fig. 1 with error bars which incorporate both systematic and statistical uncertainties. In most instances the statistical errors are smaller than or comparable to the circles and squares. For these data the principal contributions to the total errors come from a 3.6% uncertainty to the absolute efficiencies and a 7% uncertainty associated with the mean charge-state identification. Net errors obtained by combining in quadrature the above errors with rms deviations of the spectra and angular distributions from their appropriate averages range from 8% for the most extensive data to 12% for the least extensive data. For those data with substantial statistical uncertainties, larger total errors were assigned accordingly.

As can be seen in Fig. 1 the response of the excitation functions to the addition of valence neutrons is complex. The addition of valence neutrons results in large increases in subbarrier fusion. However, the excitation function for ⁵⁸Ni + ⁶⁴Ni descends more gradually than that for either ⁵⁸Ni + ⁵⁸Ni or ⁶⁴Ni + ⁶⁴Ni, and the excitation functions for ⁵⁸Ni + ⁶⁴Ni and ⁶⁴Ni + ⁶⁴Ni converge toward one another at far subbarrier energies. This behavior is in contrast to what has been observed^{7-9,14} with lighter projectiles where comparable sets of excitation functions undergo less pronounced, uniform increases at subbarrier energies.

In order to estimate how much Ni-Ni subbarrier fusion can be ascribed to simple barrier penetration, we compared our experimental results

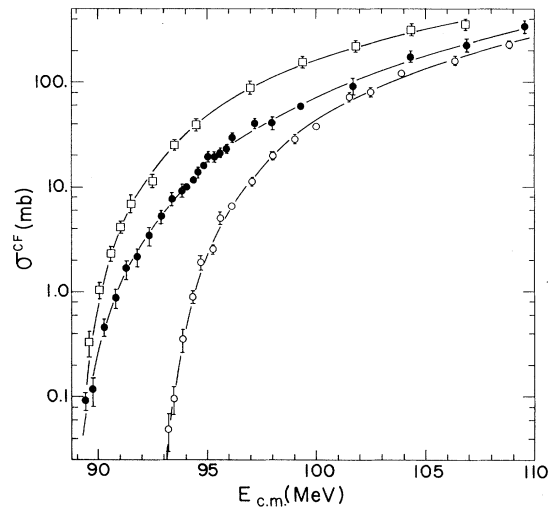


FIG. 1. Experimental cross sections for complete fusion. Squares, filled circles, and open circles denote experimental results for ⁶⁴Ni + ⁶⁴Ni, ⁵⁸Ni + ⁶⁴Ni, and ⁵⁸Ni + ⁵⁸Ni, respectively. The abscissa gives the average center-of-mass energies corrected for loss of energy in the targets taking into account the slope of the excitation functions. Smooth curves drawn through the data points are visual guides.

to those calculated in an adiabatic approach with use of Hill-Wheeler transmission coefficients

$$T_l(E_{c.m.}) = \left\{ 1 + \exp \frac{2\pi}{\hbar\omega_l} [V_l(R_l) - E_{c.m.}] \right\}^{-1}, \quad (1)$$

where V_l is the inverted harmonic oscillator potential for the l th partial wave, R_l is its radial position, and $\hbar\omega_l$ is its curvature. We did not introduce an imaginary potential but instead assumed that the nucleus is "black" (equivalent to assuming ingoing wave boundary conditions) so that we can write

$$\sigma^{CF}(E_{c.m.}) = \pi\lambda^2(E_{c.m.}) \sum_l (2l+1) T_l(E_{c.m.}), \quad (2)$$

where λ is the reduced de Broglie wavelength of the incident ion. We considered an interaction potential of the form $V(l, r) = V_N(r) + Z_T Z_P e^2 / r + \hbar^2 l(l+1) / 2\mu r^2$, where Z_T and Z_P are the target and projectile atomic numbers and μ is the reduced mass. For the nuclear potential, $V_N(r)$, we employed the generalized liquid-drop potential of Krappe, Nix, and Sierk.¹⁵ This potential is similar to the proximity potential¹⁶ and doubly folding a short-range Yukawa function over a sharp surface-density distribution takes into account both the finite-range of nuclear forces and surface diffuseness. The Hill-Wheeler quantities V_l , R_l , and $\hbar\omega_l$ were fitted with the interaction

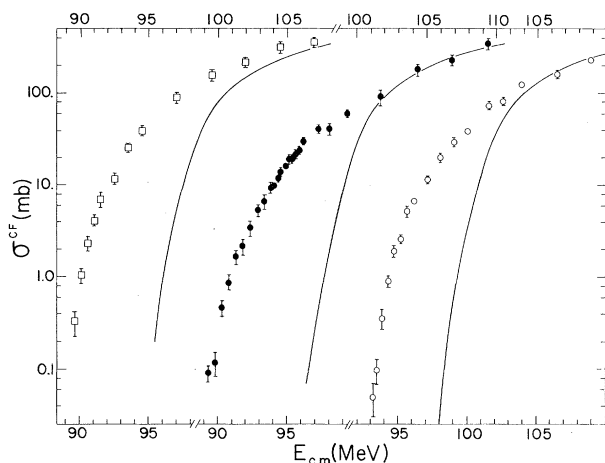


FIG. 2. Experimental and theoretical cross sections for complete fusion. Data symbols have the same meaning as in Fig. 1. Smooth curves represent generalized liquid-drop-model calculations (Ref. 15).

potential for each partial wave and σ^{CF} was calculated. Comparison of experimental and barrier-penetration-model results are shown in Fig. 2. The surprisingly large amount of subbarrier fusion not accounted for by simple barrier penetration is apparent. At above-barrier energies the experimental and calculated results are in agreement. There is some indication at the highest energies that the measured cross sections increase relative to the predicted cross sections as the number of valence neutrons increase. This may be due to single-particle effects.¹⁷

To examine to what extent the unaccounted for subbarrier fusion may be due to static deformations additional calculations were performed using the model of Wong.¹⁸ In this approach the interaction potential was expanded in terms of $\beta_2 V_{Coul}$ and the cross sections were averaged over all (planar) orientations of the two nuclei. The Ni quadrupole deformation parameters are $\beta_2(^{58}\text{Ni}) = 0.183$ and $\beta_2(^{64}\text{Ni}) = 0.166$. Since these are spherical (vibrational) nuclei these β_2 values were taken as upper limits. Preliminary calculations, which included higher-order terms such as the quadrupole-quadrupole term, were performed. It does not appear that these model calculations can reproduce the observed effects.

An alternative explanation for, at least, some of the variations in subbarrier fusion is that these variations arise from multiple-transfer or exchange processes which occur near or at the distance of closest approach and which serve as

doorways for fusion. One possibility is that valence neutrons may be exchanged to form a homopolar bond, perhaps modified by Josephson pair tunneling. Another possibility is that valence neutrons may significantly influence cross sections for reaction processes competing with fusion.

To summarize, we have measured complete-fusion excitation functions for $^{58}\text{Ni} + ^{58}\text{Ni}$, $^{58}\text{Ni} + ^{64}\text{Ni}$, and $^{64}\text{Ni} + ^{64}\text{Ni}$ at near-barrier and subbarrier energies with high precision with use of MIT-BNL velocity selector in conjunction with a gas telescope. We observed that the excitation functions for these massive systems undergo a complex response to the addition of valence neutrons. We pointed out that it is difficult to understand the behavior of these excitation functions in adiabatic, liquid-drop/static deformation terms alone. We then suggested that valence neutrons may directly and dynamically influence the fusion process in general and subbarrier penetration in particular.

The authors wish to thank Dr. H. J. Krappe for supplying the generalized liquid-drop-model calculations, Dr. C. Y. Wong for many helpful discussions, and Dr. H. E. Wegner for a critical reading of the manuscript and for the resulting suggestions. This work was supported by the U. S. Department of Energy under Contract No. AC02-76ERO3069.

^(a)Deceased.

^(b)Permanent address: Institute of Atomic Energy, Peking, People's Republic of China.

¹R. Beringer, Phys. Rev. Lett. **18**, 1006 (1967); J. Maly and J. R. Nix, in Contributions to the International Conference on Nuclear Structure, Tokyo, Japan, 1967, University of Tokyo Report, 1967 (unpublished), p. 224.

²H. Holm, W. Scheid, and W. Greiner, Phys. Lett. **29B**, 473 (1969).

³A. S. Jensen and C. Y. Wong, Phys. Rev. C **1**, 1321 (1970), and Nucl. Phys. **A171**, 1 (1971); P. W. Reisenfeldt and T. D. Thomas, Phys. Rev. C **2**, 711 (1970), and Phys. Rev. C **2**, 2448 (1970).

⁴T. Kodama, R. A. M. S. Nazareth, P. Möller, and J. R. Nix, Phys. Rev. C **17**, 111 (1978).

⁵C. Y. Wong, Phys. Lett. **26B**, 120 (1968).

⁶J. O. Rasmussen and K. Sugawara-Tanabe, Nucl. Phys. **A171**, 497 (1971); C. Y. Wong, Phys. Lett. **42B**, 186 (1972), and Phys. Rev. Lett. **31**, 766 (1973).

⁷R. G. Stokstad, Y. Eisen, S. Kaplanis, D. Pelte, U. Smilansky, and I. Tserruya, Phys. Rev. Lett. **41**, 465 (1978), and Phys. Rev. C **21**, 2427 (1980); R. G.

Stokstad, W. Reisdorf, J. H. Hildenbrand, J. V. Kratz, G. Wirth, R. Lucas, and J. Poitou, *Z. Phys. A* **295**, 269 (1980).

⁸W. Scobel, H. H. Gutbrod, M. Blann, and A. Mignerey, *Phys. Rev. C* **11**, 1701 (1975).

⁹B. Sikora, J. Bisplinghoff, W. Scobel, M. Beckerman, and M. Blann, *Phys. Rev. C* **20**, 2219 (1979).

¹⁰L. C. Vaz and J. M. Alexander, *Phys. Rev. C* **18**, 2152 (1978), and **10**, 464 (1974), and to be published.

¹¹H. Freiesleben and J. R. Huizenga, *Nucl. Phys. A* **224**, 503 (1974).

¹²H. A. Enge and D. Horn, *Nucl. Instrum. Methods* **145**, 271 (1977); M. Salomaa and H. A. Enge, *Nucl. Instrum.*

Methods **145**, 279 (1977).

¹³M. Beckerman, J. Ball, H. Enge, M. Salomaa, A. Sperduto, S. Gazes, A. DiRienzo, and J. D. Molitoris, to be published

¹⁴Y. Eyal, M. Beckerman, R. Chechik, Z. Fraenkel, and H. Stocker, *Phys. Rev. C* **13**, 1527 (1976).

¹⁵H. J. Krappe, J. R. Nix, and A. J. Sierk, *Phys. Rev. Lett.* **42**, 215 (1979), and *Phys. Rev. C* **20**, 992 (1979).

¹⁶J. Blocki, J. Randrup, W. J. Swiatecki, and C. F. Tsang, *Ann. Phys. (N.Y.)* **105**, 427 (1977).

¹⁷J. A. Nolen, Jr., and J. P. Schiffer, *Ann. Rev. Nucl. Sci.* **19**, 471 (1969), and references therein.

¹⁸C. Y. Wong, Ref. 6, and private communication.

Low-Lying Yrast States in ^{210}Rn and ^{211}Rn and the Competition between Neutron-Hole and Proton Excitations

A. R. Poletti

Department of Physics, University of Auckland, Auckland, New Zealand

and

G. D. Dracoulis and C. Fahlander

Department of Nuclear Physics, Research School of Physical Sciences, The Australian National University, Canberra, Australian Capital Territory 2600, Australia

(Received 2 June 1980)

The γ -decay and nuclear structure of low-lying yrast and near yrast levels in ^{210}Rn and ^{211}Rn have been investigated. The cascade from the yrast 6^+ state in ^{210}Rn branches to two close-lying 4^+ states, deduced to be complete mixtures of the 4^+ states arising from the proton configuration, and from the neutron-hole intruder configuration. The influence of this proton-neutron-hole interaction on the yrast cascades in ^{211}Rn and ^{206}Rn , ^{208}Rn is discussed.

PACS numbers: 23.20.Ck, 27.90.+w

Experiments which we have recently undertaken have elucidated the structure of the low-lying states of the neutron-hole isotopes ^{211}Rn and ^{210}Rn . These nuclei have four protons outside the ^{208}Pb core and, respectively, one and two neutron holes. In this Letter we wish to concentrate on the structure of the lower-lying yrast states which arise from the seniority-2, $h_{9/2}^4$ proton configuration coupled to one and two neutron holes, in the nuclei ^{211}Rn and ^{210}Rn , respectively, and to four and six neutron holes in ^{208}Rn and ^{206}Rn . Poletti *et al.*¹ have recently investigated the yrast states of ^{210}Rn , while for ^{211}Rn almost nothing of its structure has been established (Lederer and Shirley²). Information on the two lighter radon isotopes has been obtained by Ritchie³ and by Horn, Baktash, and Lister.⁴ We wish to report on a reinvestigation of the structure of the ^{210}Rn , on one aspect of the first extensive investigation

of the ^{211}Rn structure and, in particular, to draw attention to the way in which the 4^+ states from the proton and neutron-hole configurations interact.

The Australian National University 14UD Pelletron accelerator was used to excite the nuclei using the reactions $^{205}\text{Tl}(^{11}\text{B}, 5n)^{211}\text{Rn}$ and $^{205}\text{Tl}(^{10}\text{B}, 5n)^{210}\text{Rn}$, respectively, at bombarding energies near 70 MeV. As expected from nuclear structure systematics, both nuclei have a long-lived isomeric level at about 1600-keV excitation energy. In Fig. 1 we present the results of a delayed coincidence experiment for both nuclei. In the lower part of the figure we show the γ -ray spectrum delayed with respect to the 325-, 546-, 185-, and 712-keV γ -ray transitions which have already been shown (Poletti *et al.*¹) to lie above the 8^+ isomeric state at $1665 + \Delta$ keV in ^{210}Rn . Of the five γ rays shown, further analysis revealed